CLINICAL AND VACCINE IMMUNOLOGY, Aug. 2010, p. 1170–1182 Vol. 17, No. 8
1556-6811/10/$12.00 doi:10.1128/CVI.00079-10

Establishment of an Aerosol Challenge Model of Tuberculosis in Rhesus Macaques and an Evaluation of Endpoints for Vaccine Testing▽

S. A. Sharpe,[1]* H. McShane,[2] M. J. Dennis,[1] R. J. Basaraba,[3] F. Gleeson,[4] G. Hall,[1] A. McIntyre,[3] K. Gooch,[1] S. Clark,[1] N. E. R. Beveridge,[2] E. Nuth,[3] A. White,[1] A. Marriott,[1] S. Dowall,[1] A. V. S. Hill,[2] A. Williams,[1] and P. D. Marsh[1]

Health Protection Agency, Centre for Emergency Preparedness and Response, Porton Down, Salisbury, United Kingdom[1]; the Jenner Institute, University of Oxford, Oxford, United Kingdom[2]; Colorado State University, Fort Collins, Colorado[3]; and Churchill Hospital, Headington, Oxford, United Kingdom[4]

Received 2 March 2010/Returned for modification 6 April 2010/Accepted 1 June 2010

The establishment of an aerosol challenge model in nonhuman primates (NHPs) for the testing of vaccines against *Mycobacterium tuberculosis* would assist the global effort to optimize novel vaccination strategies. The endpoints used in preclinical challenge studies to identify measures of disease burden need to be accurate and sensitive enough to distinguish subtle differences and benefits afforded by different tuberculosis (TB) vaccine regimens when group sizes are inevitably small. This study sought to assess clinical and nonclinical endpoints as potentially sensitive measures of disease burden in a challenge study with rhesus macaques by using a new protocol of aerosol administration of *M. tuberculosis*. Immunological and clinical readouts were assessed for utility in vaccine evaluation studies. This is the first example of TB vaccine evaluation with rhesus macaques where long-term survival was one of the primary endpoints. However, we found that in NHP vaccine efficacy studies with maximum group sizes of six animals, survival did not provide a valuable endpoint. Two approaches used in human clinical trials for the evaluation of the gamma interferon (IFN-γ) response to vaccination (enzyme-linked immunospot [ELISpot] assay and enzyme-linked immunosorbent assay [ELISA]) were included in this study. The IFN-γ profiles induced following vaccination were found not to correlate with protection, nor did the level of purified protein derivative (PPD)-specific proliferation. The only readout to reliably distinguish vaccinated and unvaccinated NHPs was the determination of lung lesion burden using magnetic resonance (MR) imaging combined with stereology at the end of the study. Therefore, the currently proposed key markers were not shown to correlate with protection, and only imaging offered a potentially reliable correlate.

Tuberculosis (TB) is a reemerging infectious disease and is responsible for nearly 2 million deaths and 9 million new cases each year (36). The global TB pandemic has been exacerbated by the emergence of drug-resistant strains of *Mycobacterium tuberculosis*, which render treatment less effective, and by the HIV epidemic, where coinfection with HIV greatly increases the risk of reactivation of latent TB and susceptibility to active TB disease.

The most effective means of controlling this global epidemic would be by prophylactic immunization. *Mycobacterium bovis* bacille Calmette-Guérin (BCG), the only licensed TB vaccine, is administered to neonates in high-risk populations as part of the WHO Expanded Programme on Immunization. BCG consistently protects against TB meningitis and disseminated TB in childhood (27, 30), but its efficacy wanes with time, and it affords only variable protection against pulmonary disease (10). A new, more effective TB vaccine is a major global health priority and is an important part of the WHO STOP TB partnership strategy.

A large international effort is under way to develop a more effective vaccine. The leading TB vaccine development strategy involves vaccination with BCG followed by a heterologous subunit vaccine boost designed to enhance protective immunity. One such subunit vaccine is the virus-vectored subunit candidate TB vaccine developed at Oxford University, MVA85A (19) (live, replication-deficient, modified vaccinia virus Ankara [MVA] [7], expressing the highly conserved, immunodominant mycobacterial antigen 85A [Ag85A]). The enhancement of BCG with systemically administered (intradermal) MVA85A has been evaluated with several preclinical animal models and is currently the subject of ongoing evaluations in several clinical trials. This BCG-MVA85A vaccination regimen induces a high magnitude of cellular immunity in mice and cattle (19, 32) and can protect against *M. tuberculosis* in guinea pigs (34), nonhuman primates (NHPs) (31), and cattle (33). It is safe and highly immunogenic in healthy adults, adolescents, children, infants, and HIV- and *M. tuberculosis*-infected adults (6, 20, 21) and has recently entered a large-scale efficacy trial with South African infants (http://clinicaltrials.gov/ct2/show/NCT00953927).

The lack of a defined immunological correlate of protection for TB means that in order to assess efficacy, candidate TB vaccines must enter large clinical trials involving thousands of at-risk individuals in countries where the disease is endemic.

* Corresponding author. Mailing address: Health Protection Agency, Centre for Emergency Preparedness and Response, Porton Down, Salisbury, United Kingdom. Phone: 441980 612811. Fax: 441980 612731. E-mail: sally.sharpe@hpa.org.uk.

▽ Published ahead of print on 9 June 2010.

Therefore, there is a need for a validated preclinical animal model that can be utilized to accurately predict the effectiveness of a candidate vaccine in humans and to aid in the identification of correlates of protection through challenge studies. Mouse models are generally used as a first screen of vaccine candidates and are very useful for studying detailed immunological responses (24). Guinea pigs are considered a more stringent model than mice to discriminate between vaccines in terms of protective efficacy, since they show a variety of pulmonary and extrapulmonary lesion types that are similar to those observed for humans (4, 17). Although small-animal models are useful, it is widely accepted that larger animals such as cattle and NHPs are potentially the most relevant model species to predict safety, immunogenicity, and protective efficacy of vaccines prior to their large-scale evaluation in humans (8, 18). NHPs are naturally susceptible to infection with *M. tuberculosis* via the respiratory route and develop a disease that clinically closely mimics human disease. As with the other preclinical species, BCG vaccination of NHPs provides a limited level of protection against *M. tuberculosis* that can be quantified through a variety of clinical and nonclinical parameters (2, 3, 9, 12, 14).

The establishment of an aerosol challenge model in NHPs, in which the *M. tuberculosis* challenge is delivered by the same route as that which occurs during natural infection, would assist the global effort in optimizing novel vaccination strategies. The endpoints used in preclinical challenge studies to identify measures of disease burden need to be accurate and sensitive enough to distinguish subtle differences and benefits afforded by different TB vaccine regimens, including those that enhance the protective efficacy of BCG, where partial protection is already conferred and the power to detect smaller incremental improvements in small numbers of animals is limited. The aims of this study were to establish an aerosol challenge model of TB in rhesus macaques and to assess clinical and nonclinical endpoints as potentially sensitive measures of disease burden in an NHP challenge study following vaccination with BCG or BCG boosted by MVA85A. The currently most widely used challenge model with macaques uses high-dose, intratracheal administration of *M. tuberculosis*, and it has been unclear whether low-dose aerosol administration would provide a better model, because although it should replicate the route of natural infection (31), larger group sizes may be necessary to compensate for interindividual heterogeneity to a low-dose challenge (8).

MATERIALS AND METHODS

Experimental animals. The animals used in this study were rhesus macaques of Indian origin obtained from an established United Kingdom breeding colony. All animals were 4 years old at the time of challenge and naïve in terms of prior exposure to mycobacterial antigens (*M. tuberculosis* infection or environmental mycobacteria), as demonstrated by a negative tuberculin test while in their original breeding colony and by the gamma interferon (IFN-γ)-based Primagam test kit (Biocor; CSL) just prior to the start of the study. Monkeys were housed according to Home Office (United Kingdom) guidelines for the care and maintenance of primates and were sedated by intramuscular (i.m.) injection with ketamine hydrochloride (10 mg/kg of body weight) (Ketaset; Fort Dodge Animal Health Ltd., Southampton, United Kingdom) for all procedures requiring removal from their cages. All procedures involving animals were approved by the Ethical Review Committee of the Centre for Emergency Preparedness and Response, Salisbury, United Kingdom. None of the animals had been used previously for experimental procedures.

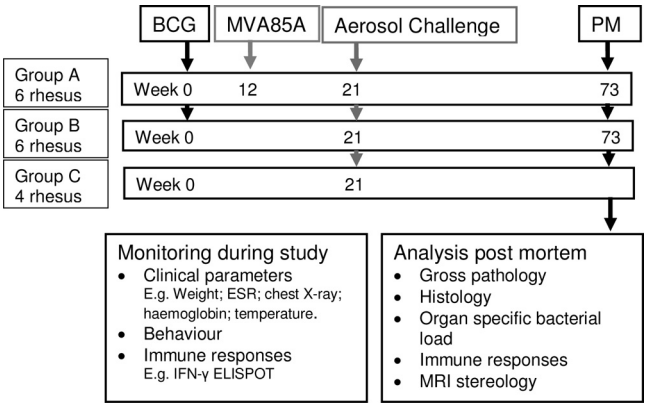

FIG. 1. Experimental study design. PM, postmortem.

Vaccination. A plan of the vaccination strategy and timing of the aerosol challenge is shown in Fig. 1. Twelve animals (groups A and B) were immunized intradermally in the upper left arm with 100 μl BCG, Danish strain 1331 (SSI, Copenhagen, Denmark). The viability of the BCG vaccine given to the NHPs was checked and found to be between 4.25×10^6 and 7.55×10^6 CFU/ml, within the expected range for the vaccine batch at 2×10^6 to 8×10^6 CFU. Twelve weeks after immunization with BCG, six animals (group A) were immunized intradermally in the upper right arm with 100 μl (5×10^8 PFU) of MVA85A. Vaccination sites were monitored and assessed for local reactions after vaccination with BCG and MVA85A.

***M. tuberculosis* challenge strain.** *M. tuberculosis* Erdman strain K 01 was kindly provided by Amy Yang (CBER/FDA). The stocks were provided as frozen suspensions at a stated titer of $3.5 \times 10^8 \pm 1.5 \times 10^8$ CFU/ml. On the day of challenge, five vials were thawed and diluted appropriately, as described below, in sterile distilled water. Twenty-one weeks after immunization with BCG, the 12 immunized animals (groups A and B) together with four unvaccinated animals (group C) were challenged by the aerosol route with *M. tuberculosis* (Fig. 1).

Aerosol exposure. The process to deliver a known number of viable *M. tuberculosis* bacilli in a target volume of inspired aerosol was performed as previously described (28). In brief, monodispersed bacteria in particles were generated by using a three-jet Collison nebulizer (BGI) and, in conjunction with a modified Henderson apparatus (11), delivered to the nose of each sedated primate via a modified veterinary anesthesia mask. Challenge was performed on sedated animals placed within a "head-out" plethysmography chamber (Buxco, Wilmington, NC) to enable the aerosol to be delivered simultaneously with the measurement of the respiration rate.

Challenge regimen. Aerosol exposure was performed over two consecutive days; groups of eight animals comprising two unvaccinated animals and three animals from each of the vaccine groups were challenged on each day.

A series of *in vitro* and *in vivo* studies were conducted in order to establish the feasibility of performing the challenge over two consecutive days, using the same initial stock suspension. These studies will be described in detail elsewhere (S. Clark et al., submitted for publication) and essentially demonstrated the following: (i) *M. tuberculosis* could be stored overnight at 4°C in the dark without a significant loss in viability, and (ii) the process of generating aerosols of *M. tuberculosis* using a Collison nebulizer resulted in an initial rapid loss of viability during the first 5 min, but after 10 min, the viability remained stable for approximately 20 min of continuous aerosolization. To avoid the initial, highly variable fluctuation in viability and to ensure that each individual exposure occurred during the period of stable viability, a strategy was developed where a 10-min "pretreatment" of the challenge suspension was performed.

On the day of challenge, five vials of Erdmann strain K 01 were thawed, pooled, and diluted 1:60 in sterile distilled water to a total volume of 200 ml, which was split into two 100-ml aliquots. One aliquot was used immediately to challenge eight animals, and the second aliquot was stored at 2°C to 8°C in the dark for the challenge of the remaining eight animals on the second day. At the start of each challenge day, one 100-ml aliquot of the mycobacterial suspension was "pretreated" in the Collison nebulizer for 10 min and then divided into eight aliquots each of 12.5 ml, which were stored at room temperature in the dark until use. A fresh aliquot of pretreated Erdman was used to challenge each animal. Animals were sedated with a combination of ketamine-acepromazine (ACP)-atropine (100 mg/ml ketamine [Ketaset; Fort Dodge Animal Health, Southamp-

TABLE 1. Aerosol challenge doses of *M. tuberculosis* delivered to rhesus macaques

Vaccine group (regimen)	Animal	Presented dose (CFU)	Estimated retained dose (CFU)
A (BCG + MVA85A)	K20	1,293	60
	K61	898	40
	K65	1,271	60
	K69	858	40
	K79	1,299	60
	K86	812	40
B (BCG)	K43	1,263	60
	K44	1,368	65
	K50	932	45
	K52	1,275	60
	K59	884	40
	K80	817	40
C (no vaccine)	K32	1,286	60
	K47	1,237	60
	K54	821	40
	K62	821	40

ton, United Kingdom], 10 mg/ml ACP [Novartis], and 0.6 mg/ml atropine sulfate [Martindale Pharmaceuticals, Romford, United Kingdom]) in a ratio of 5:1:1 and then exposed to the aerosol of *M. tuberculosis* for sufficient time (4 to 10 min) for the inhalation of an acquired volume of 7 liters. Macaques were challenged with estimated doses of 40 to 60 CFU retained in the lungs (Table 1).

Clinical assessment postchallenge. Animal behavior was observed daily throughout the study for contraindicators such as depression, withdrawal from the group, aggression, food and water intake, changes in respiration rate, or cough. Animals were sedated every 2 weeks to measure weight, body temperature, blood hemoglobin levels, and erythrocyte sedimentation rate (ESR) and to collect blood samples for immunology. Blood cell hemoglobin was measured by using a HaemaCue hemoglobinometer (HaemaCue Ltd., Dronfield, United Kingdom), and the ESR was measured by using the Sediplast system (Guest Medical, Edenbridge, United Kingdom). The time of necropsy, if prior to the end of the planned study period, was determined by experienced primatology staff based on a combination of the following adverse indicators: depressed or withdrawn behavior, abnormal respiratory rate (dyspnea), loss of 20% of peak postchallenge weight, ESR level elevated above normal, hemoglobin level below normal limits, increased temperature, and severely abnormal chest X ray.

IFN-γ enzyme-linked immunospot (ELISpot) assay. Peripheral blood mononuclear cells (PBMC) were isolated from heparin-anticoagulated blood by Ficoll-Hypaque Plus (GE Healthcare, Buckinghamshire, United Kingdom) density gradient separation using standard procedures. Isolated cells were washed in medium (R2) consisting of RPMI 1640 medium (Sigma-Aldrich, Dorset, United Kingdom) supplemented with L-glutamine (2 mM) (Sigma-Aldrich, Dorset, United Kingdom), penicillin (50 U/ml)-streptomycin (50 μg/ml) (Sigma-Aldrich, Dorset, United Kingdom), 25 mM HEPES buffer (Sigma-Aldrich, Dorset, United Kingdom), 0.05 mM 2-mercaptoethanol (Invitrogen, Paisley, United Kingdom), and 2% heat-inactivated fetal bovine serum (LabTech, Ringmer, England).

An IFN-γ ELISpot assay was used to estimate the numbers and IFN-γ production capacity of mycobacterium-specific T cells in PBMC using a human/monkey IFN-γ kit (MabTech, Nacka, Sweden). Cells were stimulated with purified protein derivative (PPD) (10 μg/ml; SSI, Copenhagen, Denmark) or pools of overlapping 15-mer peptides spanning Ag85A or ESAT6 (Peptide Protein Research Ltd., Wickham, United Kingdom). Plates (Millipore, Watford, United Kingdom) were coated overnight at 4°C with 10 μg/ml of IFN-γ antibody. A total of 200,000, 100,000, or 5,000 PBMC were plated per well in 100 μl R5 medium (RPMI 1640 medium supplemented with L-glutamine [2 mM], penicillin [50 U/ml]-streptomycin [50 μg/ml], and 5% heat-inactivated fetal bovine serum), with or without antigen, in triplicate and incubated for 18 h. Phorbol-12-myristate (100 ng/ml; Sigma-Aldrich Dorset, United Kingdom) and ionomycin (1 μg/ml; CN Biosciences, Nottingham, United Kingdom) were used as a positive control. After culture, plates were washed and incubated for 2 h with biotinylated anti-IFN-γ. Spots were developed by the addition of streptavidin-alkaline phosphatase and freshly prepared 5-bromo-4-chloro-3-indolyl phosphate (BCIP)–Nitro Blue tetrazolium (NBT) substrate. Determinations from triplicate tests were averaged. Data were analyzed by subtracting the mean number of spots in the cells and medium-only control wells from the mean counts of spots in wells with cells and antigen or peptide pools.

Quantification of secreted IFN-γ. IFN-γ production was measured by using a whole-blood enzyme-linked immunosorbent assay (ELISA) as described previously by Black et al. (5). In brief, heparinized blood was diluted 1 in 10 with serum-free medium (RPMI medium supplemented with L-glutamine, penicillin, and streptomycin) and cultured with PPD from *M. tuberculosis* (5 μg/ml; SSI, Copenhagen, Denmark) or mitogen phytohemagglutinin (PHA) (5 μg/liter; Sigma-Aldrich, Dorset, United Kingdom) or in medium alone for 6 days. Supernatants were harvested at day 6 and stored at −20°C. The quantity of IFN-γ in the supernatants was estimated by using a commercially available human/monkey IFN-γ ELISA kit (MabTech, Nacka, Sweden). Purified human IFN-γ was used for the standard curve on each plate. The ELISA was developed by using streptavidin and the 3,3′,5,5′-tetramethylbenzidine (TMB) liquid substrate system (Sigma-Aldrich, Dorset, United Kingdom), and the reaction was stopped with 2 M sulfuric acid (May & Baker Ltd., Dagenham, United Kingdom). ELISA plates were read at 450 nm. A standard curve was plotted for each plate and used to calculate the concentrations of IFN-γ in each sample.

Intracellular cytokine staining. Freshly isolated PBMC were stimulated with either phosphate-buffered saline (PBS) (negative control), PPD, or staphylococcus enterotoxin B (SEB) (Sigma, Poole, United Kingdom) at 10 μg/ml with 0.1 μg/ml of purified anti-CD28 and 0.1 μg/ml of purified anti-CD49d (both BD Biosciences, Oxford, United Kingdom). Cells were incubated at 37°C for 5 h. Golgiplug (BD Biosciences, Oxford, United Kingdom) was added, and cells were incubated for a further 12 h at 37°C. Cells were stained for the expression of $CD8^+$, $CD3^+$, $CD4^+$, and IFN-γ by using standard commercially available fluorochrome-conjugated reagents (BD Biosciences, Oxford, United Kingdom, and Caltag Invitrogen, Paisley, United Kingdom) acquired on an FC500 Cytomics flow cytometer (Beckman Coulter, High Wycombe, United Kingdom) and analyzed by using CXP V2.1 software (Beckman Coulter, High Wycombe, United Kingdom).

Polyfunctional intracellular cytokine staining. PBMC were thawed; washed; resuspended in medium (R10) consisting of RPMI 1640 medium supplemented with L-glutamine (2 mM), penicillin (50 U/ml)-streptomycin (50 μg/ml), and 10% heat-inactivated fetal bovine serum with 1 U/ml of DNase (Sigma, Poole, United Kingdom); and incubated at 37°C. After 2 h, the cell concentration was adjusted to 1×10^6 cells/ml in R10 medium containing 1 μg/ml of anti-CD28 (BD Biosciences, Oxford, United Kingdom), 1 μg/ml of anti-CD49d (BD Biosciences, Oxford, United Kingdom), and 10 μg/ml of brefeldin A (Sigma, Poole, United Kingdom). PBMC were stimulated with one of the following: 10 μg/ml PPD (SSI, Copenhagen, Denmark), 2 μg/ml antigen 85A complete peptide pool (66 15-mer peptides overlapping by 10 amino acids; 2-μg/ml final concentration for each amino acid), BCG at 1×10^6 CFU, or 5 μg/ml of SEB (Sigma, Poole, United Kingdom). Unstimulated PBMC were used to assess nonspecific cytokine production. Cells were incubated at 37°C with 5% CO_2 in air for 10 h. Following stimulation, PBMC were washed in PBS containing 0.1% bovine serum albumin (BSA) and 0.01% sodium azide (both Sigma, Poole, United Kingdom) by centrifugation at $400 \times g$ for 5 min. Following a second wash step, cells were stained with the amine-reactive Live/Dead Fixable Red Dead cell stain kit (Molecular Probes, Invitrogen, Paisley, United Kingdom) and labeled with the following antibodies at optimally diluted concentrations: $CD4^+$-phycoerythrin (PE), $CD8^+$-PE-Cy7 (BD Biosciences, Oxford, United Kingdom), CD14-phycoerythrin-Texas Red, and CD20-phycoerythrin-Texas Red (Beckman Coulter, High Wycombe, United Kingdom). After labeling for 30 min with light excluded, cells were washed by centrifugation before permeabilization by incubation at room temperature for 15 min with Fix/Perm (BD Biosciences, Oxford, United Kingdom). PBMC were washed by centrifugation at $400 \times g$ for 5 min with Permwash (BD Biosciences, Oxford, United Kingdom) and then labeled with CD3-allophycocyanin (APC)-C7 (to account for downregulation after stimulation) and also the following cytokines: IFN-γ–fluorescein isothiocyanate (FITC) (both BD Biosciences, Oxford, United Kingdom), tumor necrosis factor alpha (TNF-α)-Pacific blue (eBiosciences, Hatfield, United Kingdom), and IL-2–APC (Miltenyi Biotech, Bisley, United Kingdom).

Flow cytometric acquisition of polyfunctional intracellular cytokine staining samples. Cells were analyzed by using a three-laser standard LSRII instrument (BD Biosciences, Oxford, United Kingdom). Cytokine-secreting T cells were identified by using a forward-scatter-height (FSC-H) versus side-scatter-area (SSC-A) dot plot to identify the lymphocyte population to which appropriate gating strategies were applied to exclude doublet events, nonviable cells, monocytes ($CD14^+$), and B cells ($CD20^+$) prior to sequential gating through histograms of $CD3^+$, $CD8^-$, and $CD4^+$ versus IFN-γ and $CD3^+$, $CD8^+$, and $CD4^-$

versus IFN-γ. The Boolean gate platform was used with individual function gates to create all response pattern combinations. Data for subsequent analyses were prepared by using Pestle, version 1.6.1 (Mario Roederer, Vaccine Research Center, NIAID, NIH), and SPICE, version 4 (Mario Roederer, Vaccine Research Center, NIAID, NIH), was used to calculate threshold and present experimental results.

Lymphoproliferation assay. A conventional tritiated thymidine proliferation assay was performed. Briefly, PBMC were cultured in triplicate at 1×10^5 cells/well in 96-well plates with medium alone or in the presence of PPD at concentration ranges of 1, 5, and 10 μg/ml for 7 days or concanavalin A (10 μg/ml; Sigma) for 3 days. [^{3}H]thymidine (GE Healthcare, Little Chalfont, United Kingdom) was added at 1 μCi/well for 6 h, cells were harvested, and thymidine uptake was measured by using a β-counter (Tri-Carb 2900TR liquid scintillation analyzer; Packard Biosciences Company, Perkin-Elmer, Milano, Italy). The proliferative capacity was expressed as the stimulation index (SI) (mean [^{3}H]thymidine incorporation of cells stimulated with antigen/mean incorporation in the absence of stimulation, i.e., medium alone).

Necropsy. Before necropsy, animals were sedated with ketamine (15 mg/ml i.m.), weighed, and photographed; chest X-rays were taken; clinical data were collected; and exsanguination was effected via the heart before termination by the injection of a lethal dose of anesthetic (Dolelethal, 140 mg/kg; Vétoquinol UK Ltd.). A full necropsy was performed, and gross pathology was scored by using a relative scoring system based on the number and extent of lesions present in lungs, spleen, liver, kidney, and lymph nodes as previously described (28). Samples of spleen, liver, kidneys, and hilar, inguinal, and axillary lymph nodes were removed; dissected on sterile trays; and placed into weighed tubes for quantitative bacteriology and into formalin-buffered saline for histology. The whole lungs were carefully dissected to retain their integrity. Following examination, the left bronchus of the lung was clamped off using artery forceps, and the left upper and left lower lung lobes were dissected away from the lung. The upper and lower left lobes were collected for quantitative bacteriology. The left bronchus was tied off with string to the left of the clamp, and the right-hand side of the lung was gently infused with 10% neutral buffered formalin using a 10-ml syringe attached to a 14 CH Netalon catheter (JAK Marketing, York, United Kingdom) while observing closely for inflation. The trachea was tied off, and the lungs were immersed in formalin to complete fixation.

Lung imaging. Thoracic radiographs (SP VET 3.2; Xograph Imaging Systems Ltd.) were acquired by using mammography film (Xograph Imaging Systems Ltd., Tetbury, United Kingdom) before and every 2 weeks after exposure to *M. tuberculosis*. Evaluation of disease was performed by an experienced consultant thoracic radiologist blinded to the animal group and clinical status by using a predetermined scoring system based on the amount and distribution of infiltrate (28).

MRI. The inflated lungs that had been immersed in formalin were set in agarose for magnetic resonance (MR) imaging (MRI) scanning. Images were acquired on a 1.5-T Twinspeed HDX MRI scanner (General Electric Healthcare, Milwaukee, WI). The sample was placed into a general-purpose flexible coil. T1-weighted three-dimensional (3D) fast spoiled gradient echo (FSPGR) images were acquired with the following parameters: time to repetition (TR), 7.7 time to echo (TE) 4.2, 16-cm field of view, 1-mm slice thickness, −0.5-mm slice gap, 192-by-192 matrix, 15° flip angle, and, number of excitations (NEX) 3. Each acquisition took approximately 3.5 min.

Lesion analysis/quantification (stereology). Lung lesions were identified on MR images based on their signal intensity and nodular morphology relative to more-normal lung parenchyma. The total lung and lesion volume relative to that of the fixed tissue was determined by using the Cavalieri method applied to MRI stacks and then expressed as a ratio to provide a measure of disease burden in each animal, as previously described (28). Analyses of lesion volume on MR images were performed with the investigators reading the images blind to treatment groups.

Pathology/histology. Upon return from scanning, lung lobes were removed from agar and stored in pots of 10% neutral buffered formalin. Lung lobes that had been fixed in buffered formalin were sliced at approximately 5- to 10-mm intervals, and discrete lesions measuring 1 to 5 mm in diameter were counted. Lesions that had coalesced and measured more than 5 mm in diameter were counted, and the dimensions of the sectioned coalesced lesions were measured and recorded. The total lesion count was the sum of the discrete and coalesced lesions. Lesions were classified according to the scheme described previously by Lin et al. (16).

Bacteriology. The left lung lobes were sampled for the presence of viable *M. tuberculosis* bacteria postmortem. The weights of all samples were determined. Lung lobes (1.97 to 16.25 g) were homogenized in 10 ml, and sections of spleen (0.072 to 2.54 g), liver (0.38 to 2.61 g), kidney (0.011 to 2.39 g), and hilar lymph nodes (0.317 g) were sampled and homogenized in 2 ml of sterile water. All samples were either serially diluted in sterile water prior to being plated or plated directly onto Middlebrook 7H11 oleic acid-albumin-dextrose-catalase (OADC) selective agar. All plates were incubated for 3 weeks at 37°C, and the resultant colonies were counted.

Statistical analyses. To compare the immune response profiles induced in animals by vaccination or challenge, the area under the curve (AUC) for each response was calculated by using Sigmaplot, version 10 (Systat Software Inc., Hounslow, United Kingdom), for each animal. The areas under the curves calculated for the animals in each test group were compared to those for the animals in other test groups with a Mann-Whitney test using Minitab, version 15 (Minitab Ltd., Coventry, United Kingdom).

Differences in the survival rates of animals in each test group were compared with a log rank test using Minitab, version 15. A Cox regression analysis was performed in order to estimate the hazard ratios and 95% confidence intervals using STATA statistical software 2007, release 9.2 (StataCorp LP, TX).

The Spearman correlation test was used to determine the level of correlation between study parameters using GraphPad Prism, version 5.01 (GraphPad Software Inc., La Jolla, CA).

RESULTS

IFN-γ response to vaccination. The mycobacterium-specific IFN-γ response was measured by an ELISpot assay (Fig. 2A and B), whole-blood ELISA (Fig. 2C), and intracellular cytokine staining (Fig. 2D). All three assays (Fig. 2A, C, and D) revealed similar response profiles, with low levels of PPD-specific IFN-γ responses after vaccination with BCG. Statistical analysis using AUC and Mann-Whitney tests confirmed significant differences in PPD-specific responses between BCG-vaccinated animals in groups A and B and unvaccinated animals in group C ($P = 0.01$ for group A versus group C and $P = 0.01$ for group B versus group C by ELISpot; $P = 0.025$ for group A versus group C and $P = 0.013$ for group B versus group C by ELISA).

Although an increase in the PPD-specific response was seen in two of the six animals (animals K65 and K86) that received the MVA85A booster vaccine, 1 week after immunization, a comparison of the AUCs of the PPD response between week 12 (time of MVA85A vaccination) and week 20 (just prior to challenge) using Mann-Whitney tests did not reveal significant differences in the immune profiles induced in the whole group of animals that received BCG alone (group B) or those that received BCG followed by MVA85A (group A) (Fig. 2A and C). However, the levels of responses in both group A and group B were significantly greater than those in the unvaccinated control group ($P = 0.04$ for group A versus group C and $P = 0.04$ for group B versus group C by ELISpot; $P = 0.011$ for group A versus group C and $P = 0.014$ group B versus group C by ELISA) by performing Mann-Whitney tests on AUC analyses of the same time period.

There were no significant differences in the profiles of the responses to Ag85A made by vaccinated and unvaccinated animals after vaccination with BCG (Fig. 2A). After vaccination with MVA85A, the response profile for group A, which received the booster vaccination, was found to be significantly different from profiles for both the unvaccinated group, group C ($P = 0.04$), and the group vaccinated with BCG alone, group B ($P = 0.02$), using AUC analysis and Mann-Whitney tests from weeks 12 to 20.

Polyfunctional T-cell responses following vaccination. The cytokine responses made by antigen-specific T-cell populations isolated from animals in the period following vaccination were

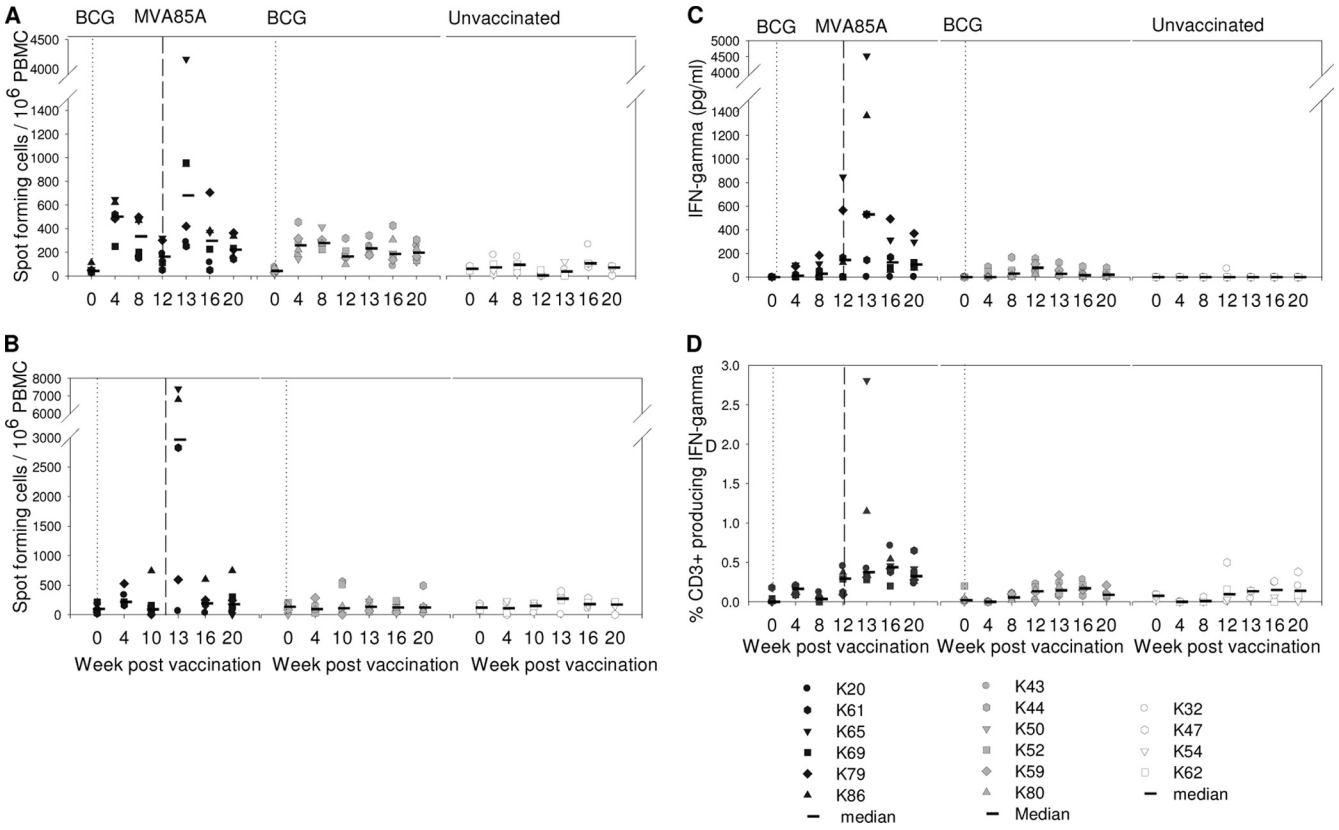

FIG. 2. Immune response to vaccination. (A) Frequency of PPD-specific IFN-γ-secreting cells measured by ELISpot assay. (B) Frequency of Ag85A-specific IFN-γ-secreting cells measured by ELISpot assay. (C) Quantity of IFN-γ secreted by PBMC during 6 days of culture of PBMC with PPD measured by ELISA. (D) Frequency of $CD3^+$ T cells that secreted IFN-γ following stimulation with PPD. Vaccination with BCG at week 0 is indicated by the dotted line, and vaccination with MVA85A indicated by the dashed line at week 12.

further investigated by using multiparameter flow cytometry. The $CD4^+$ and $CD8^+$ T-cell populations were evaluated for their capabilities to produce IFN-γ, IL-2, and TNF-α, either individually (single-positive cells) or in combination (double- and triple-positive cells) prior to vaccination with BCG on the day of MVA85A vaccination and then 1, 2, and 8 weeks after MVA85A vaccination.

Ag85A-specific single-, double-, and triple-positive $CD4^+$ T cells were detected only in animals that received vaccination with MVA85A (Fig. 3C). There was considerable heterogeneity between animals within each group. Raised levels of single-, double-, and triple-positive IFN-γ-secreting cells were seen in animals K65 and K86 1 week after vaccination with MVA85A. Ag85A-specific IFN-γ-secreting $CD4^+$ T cells were not detected in animal K20, K61, or K79 after vaccination with MVA85A (Fig. 3A). IL-2^+ IFN-γ^+ and IL-2^+ TNF-α^+ double-positive Ag85A-specific $CD4^+$ T-cell responses were not seen at levels above those measured prior to vaccination in any of the animals in the study (data not shown). Through all experimental groups, the production of IL-2 was either low relative to IFN-γ or TNF-α or not detected.

A number of PPD-specific cytokine-producing $CD4^+$ T-cell populations were detected in vaccinated animals at levels above those seen prior to vaccination in the period between MVA85A vaccination and challenge. However, the functional profiles did not differentiate between animals vaccinated with BCG alone or animals on the BCG-MVA85A regimen. Single-positive PPD-specific, TNF-α-secreting $CD4^+$ T cells were seen at levels above those seen before immunization, during the period after vaccination with MVA85A (study weeks 13 to 20), in three animals that received the BCG-MVA85A vaccine regimen (animals K79, K61, and K86) and two animals that received the BCG vaccine alone (animals K52 and K43) but not in any of the unvaccinated animals (Fig. 3E). Similarly, an increase in levels of PPD-specific IFN-γ-producing $CD4^+$ T cells was detected in animals K69, K86, and K79 from the BCG-MVA85A-vaccinated group and animal K43 from the BCG-only-vaccinated group (Fig. 3D). An increase in levels of double-positive (IL-2^+ TNF-α^+) PPD-specific $CD4^+$ T cells was detected in two animals (animals K79 and K86) 1 week after MVA85A vaccination and in one animal (animal K43) from the group vaccinated with BCG alone during the same period (Fig. 3G) at week 20. Increases in levels of double-positive IFN-γ^+ TNF-α^+ (Fig. 3E) and triple-positive PPD-specific $CD4^+$ T cells (Fig. 3H) were seen 1 week after MVA vaccination in three animals (animals K65, K79, and K86). Levels of single-positive IL-2^+- and double-positive IFN-γ^+ IL-2^+-secreting PPD-specific $CD4^+$ T-cell responses did not increase in either vaccinated or unvaccinated animals (data not shown). Neither double- nor triple-positive PPD nor Ag85A-specific $CD8^+$ T cells were detected in animals in this study, although some IFN-γ^+ and IL-2^+ single-positive responses

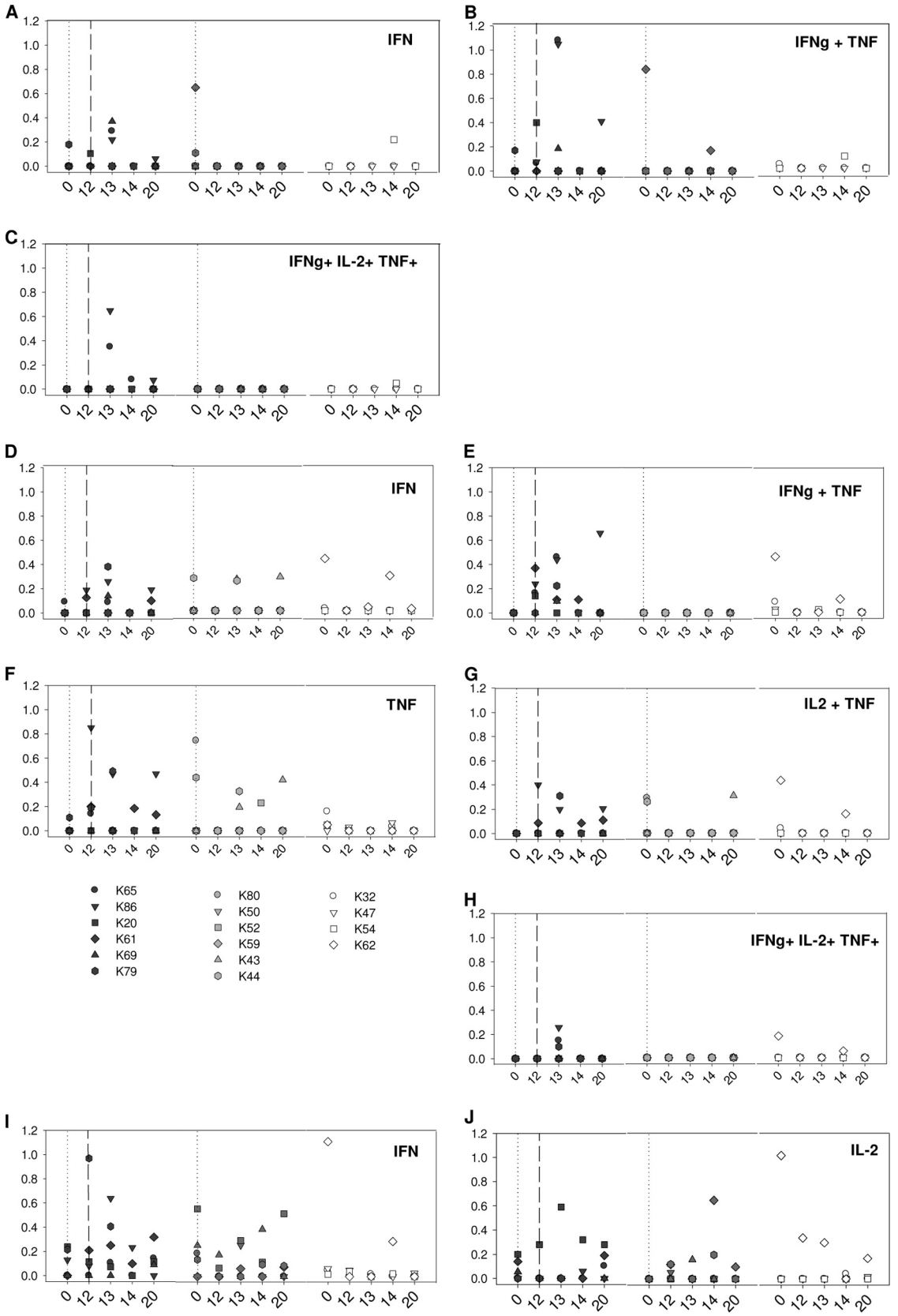

FIG. 3. Polyfunctional T-cell analysis after vaccination. (A to C) Responding $CD4^+$ T-cell populations following stimulation with Ag85A peptide pools. (D to H) Responding $CD4^+$ T-cell populations following stimulation with PPD. (I and J) Responding $CD8^+$ T cells following stimulation with PPD.

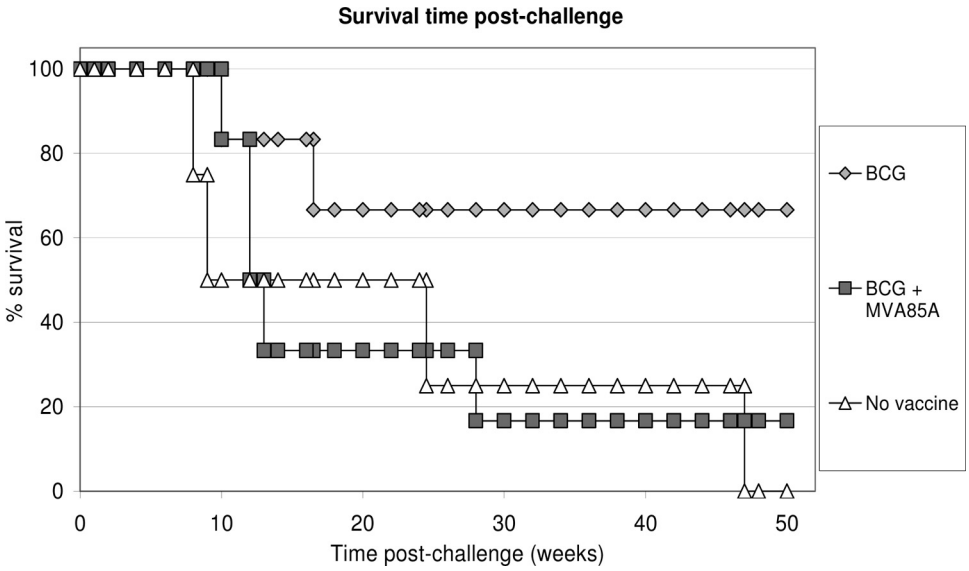

FIG. 4. Kaplan-Meier plot of survival of vaccinated and unvaccinated NHPs after challenge with *M. tuberculosis*.

were seen (IFN-γ for animals K86, K79, and K61 in the BCG-MVA group and animal K43 in the BCG group, and IL-2 for animal K20 in the BCG-MVA group, animals K43, K44, and K59 in the BCG group, and animal K62 in the unvaccinated group) (Fig. 3I and J).

Proliferative responses following vaccination. T-cell recognition and response to PPD stimulation were investigated by using a standard tritiated thymidine incorporation assay. In the group that received the BCG-MVA85A vaccination regimen, all animals made low PPD-specific proliferative responses (SI $<$ 20) in the period after BCG vaccination and before vaccination with MVA85A (weeks 0 to 12). Response levels increased after vaccination with MVA85A (SI range, 40 to 60) in two of the six animals (animals K65 and K69). All six animals in the group that received only the BCG vaccine made PPD-specific proliferative responses during the period before challenge. The largest responses were seen for animal K44 (SI range, 20 to 80); in contrast, responses in the other five animals were much lower (SI $<$ 10) (data not shown). Statistical analysis using AUC and Mann-Whitney tests did not demonstrate a significant difference in PPD-specific responses made by animals vaccinated with BCG and MVA85A (group A) and those vaccinated with BCG alone (group B), either after vaccination with BCG (weeks 0 to 12) or during the period after MVA85A vaccination and challenge (weeks 12 to 20).

Clinical status following vaccination. All animals in the study showed the weight gain profiles expected for healthy animals during the period prior to challenge. Temperature, erythrocyte sedimentation rate (ESR), and hemoglobin levels all remained within the normal range during the vaccination phase of the study. Local skin reactions at the site of BCG immunization were seen for all vaccinated animals. Reactions appeared 2 to 4 weeks after BCG vaccination in 10 of 12 immunized animals but resolved in all animals 22 weeks after immunization. A local skin reaction at the site of immunization was seen for all six animals vaccinated with MVA85A. Reactions peaked 1 week after vaccination and had resolved 8 weeks after immunization for all animals. Vaccination with MVA85A also induced an increase in the size of axillary lymph nodes draining the site of vaccination for all animals following vaccination with MVA85A. Maximum lymph node size was seen 1 to 2 weeks after immunization and returned to normal in all animals 6 to 8 weeks after vaccination.

Changes in clinical parameters following aerosol challenge with *M. tuberculosis*. Animals in all three study groups showed changes in behavior and clinical parameters consistent with a progression of tuberculosis-induced disease and were euthanized when set humane endpoints were reached ahead of the planned end of the study. Disease progressed to reach humane endpoints in all four animals in naïve control group C (animals K32, K47, K54, and K62), two of six BCG-vaccinated animals in group B (animals K44 and K52), and five of six BCG-MVA85A-vaccinated animals in group A (animals K20, K61, K69, K79, and K86) (Fig. 4).

All animals that met humane endpoints showed a range of clinical signs in the 5 days before euthanasia. These signs included depression and withdrawal from the group. Abnormal rapid respiration rates and shallow, labored breathing were also observed for this group, and coughing was observed for all animals except animal K32. Ruffled fur was seen for four animals (animals K20, K32, K54, and K61). In the period prior to termination, all the animals that met humane-endpoint criteria showed progressive weight loss and elevated ESRs (Fig. 5F and G). At termination, all the unvaccinated animals (animals K32, K47, K54, and K62), one of six BCG-vaccinated animal (animal K52), and two of six BCG-MVA85A-vaccinated animals (animals K61 and K69) showed erythrocyte hemoglobin concentrations below the normal range. No adverse clinical or behavioral indicators were exhibited by BCG-vaccinated animals K43, K50, and K59 or BCG-MVA85A-vaccinated animal K65 at the time of termination 52 weeks after challenge.

Pulmonary abnormalities were identified on X radiographs from all animals after challenge and remained until the end of the study period. Abnormalities were not detected until 4

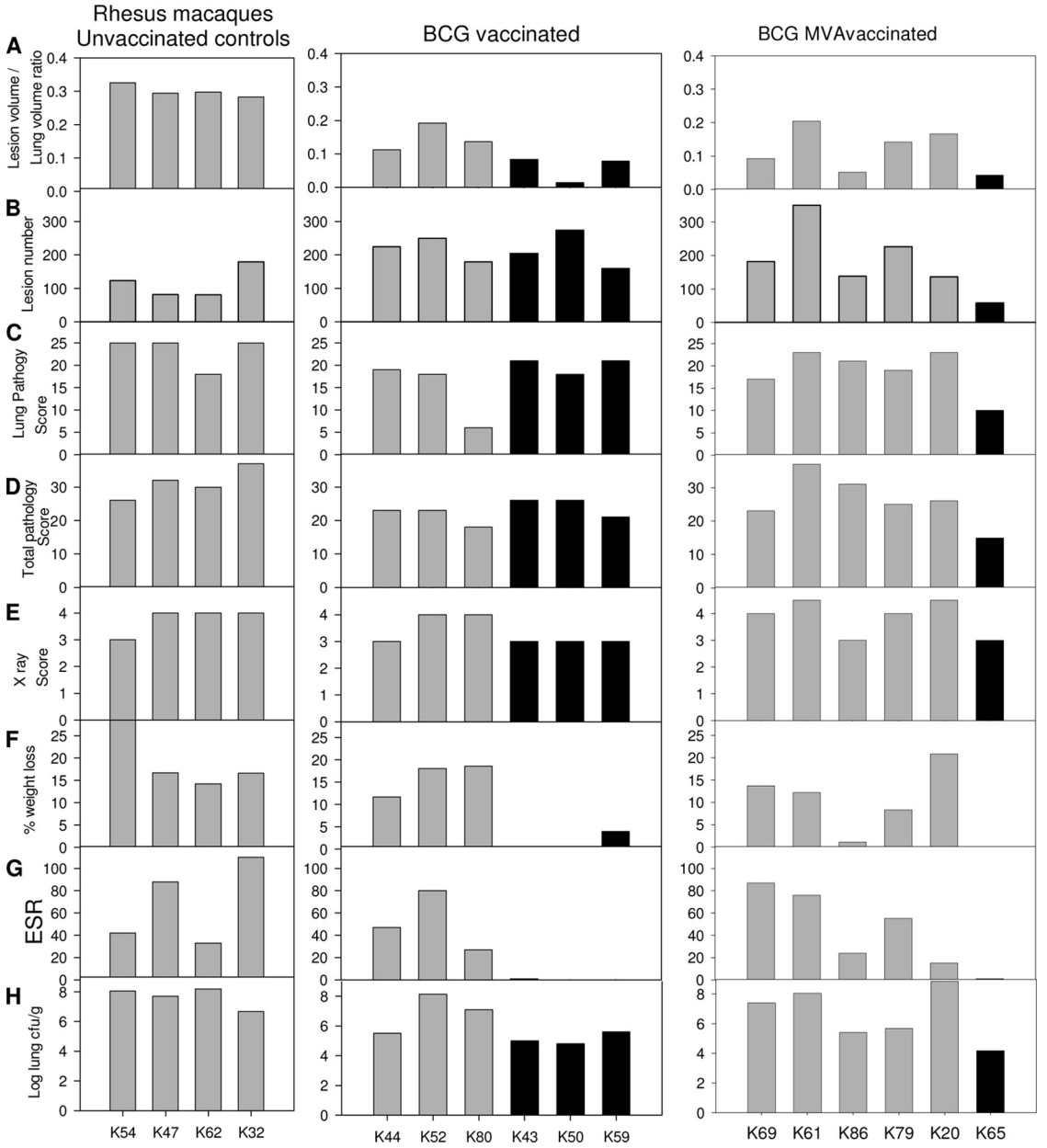

FIG. 5. Measures of tuberculosis-induced pulmonary and clinical disease burden. (A) Ratio of lung volume to lesion volume determined by MR stereology. (B) Number of lesions in the lung enumerated by serial sectioning and manual counting. (C) Total pathology score determined by using a qualitative scoring system. (D) Scores attributed to the pulmonary component as part of the total pathology score. (E) Score attributed to the chest radiogram on the day of euthanasia. (F) Percent weight loss from peak postchallenge weight on the day of euthanasia. (G) ESR on the day of euthanasia. (H) Bacterial load in the lung.

weeks after challenge for any of the animals, at which point infiltrates were detected on both sides of the lung (score of 3) in all except two animals, animals K86 and K59, where the detection of bilateral infiltration was delayed until weeks 12 and 28, respectively. Infiltrates were extensive (score of 4) by the time of euthanasia for three of the four control animals (animals K32, K47, and K62), two BCG-vaccinated animals (animals K52 and K80), and four of the BCG-MVA85A-vaccinated animals (animals K20, K61, K69, and K79) (Fig. 5E). Calcified nodules were observed on radiographs taken from week 24 after challenge onwards for all the animals that remained clinically healthy during the study. Calcified nodules were first identified at week 24 in animal K65, week 30 in animals K43 and K80, week 34 in animal K50, and week 38 in animal K59.

Survival postchallenge. The lengths of time that animals in each group survived before disease progressed to reach clinical endpoints were compared by using two statistical approaches, the log rank test and Cox regression analysis. Both approaches showed no overall difference in survival time postchallenge between the three groups ($P = 0.13$ by log rank test, and $P = 0.093$ by Cox regression).

TABLE 2. Statistical analysis of the differences between test groups using different vaccine efficacy readouts[a]

Readout	*P* value		
	Unvaccinated vs BCG	Unvaccinated vs BCG-MVA85A	BCG vs BCG-MVA85A
Ratio of lesion vol to lung vol	0.011[b]	0.011[b]	0.631
No. of lesions	0.024[c]	0.199	0.337
Total pathology score	0.017[b]	0.198	0.33
Lung pathology score	0.079	0.083	0.466
Chest X ray	0.174	0.285	0.371
Bacterial load (CFU/g)	0.136	0.522	0.297
% wt loss	0.199	0.055	0.747
ESR	0.087	0.157	0.515

[a] Mann-Whitney test results are shown.
[b] Vaccinated significantly lower than unvaccinated ($P < 0.05$).
[c] Vaccinated significantly higher than unvaccinated ($P < 0.05$).

Survival times were then compared between each of the vaccination groups A and B and unvaccinated control group C. The survival of BCG-vaccinated animals was found to be significantly different from that of the unvaccinated control animals using the Kaplan-Meier log rank test ($P = 0.048$) but not significantly different using Cox regression ($P = 0.07$). No difference in the survival times was seen between the group vaccinated with BCG alone and the group vaccinated with BCG followed by MVA85A by either test ($P = 0.1$ by log rank test, and $P = 0.17$ by Cox regression).

Measures of tuberculosis-induced pulmonary and extrapulmonary disease burden. At the end of the study the level of tuberculosis-induced pulmonary and clinical disease was investigated by using quantitative and qualitative approaches (Fig. 5). The pulmonary disease burden was quantified by using stereology on MR images to determine the total lesion volume and the total lung volume and then expressed as a ratio of lesion volume to lung volume. A significant difference in the ratio of lesion volume to lung volume was seen between the unvaccinated control animals and animals vaccinated with BCG alone or with BCG boosted with MVA85A (Fig. 5A and Table 2), with both groups of vaccinated animals having a lower ratio than the controls. The ratio of lesion volume to lung volume was not significantly different between the BCG- and BCG-MVA85A-vaccinated groups. The ratio of lesion volume to lung volume was lower in animals that did not show adverse clinical indicators at termination (animals K65, K43, K50, and K59).

The pulmonary disease burden was also quantified by serial sectioning and manual counting of both discrete and coalesced lesions (Fig. 5B). Lesion numbers were not significantly different between the unvaccinated and the BCG-MVA85A-vaccinated animals or the BCG-vaccinated and the BCG-MVA85A-vaccinated groups. However, a significantly higher number of lesions was seen in the BCG-vaccinated animals than in the unvaccinated animals (Table 2).

The distribution and type of pulmonary granulomas (classified according to a scheme described previously by Lin et al. [16]) identified in sections of lung did not distinguish between the different groups, nor did this predict survival, and neither did disease spread to extrapulmonary tissues measured by lesion presence in hilar lymph node, liver, kidney, and spleen. Histological examination revealed granulomas in extrapulmonary tissues in all four of the unvaccinated animals; three of the six BCG-vaccinated animals (animals K43, K50, and K59), all of which remained clinically well until the end of study; and four of the six BCG-MVA85A-vaccinated animals (animals K86, K61, K69, and K20), all of which succumbed to disease during the study.

The pulmonary disease burden was also measured by using qualitative approaches conventionally used for the evaluation of TB vaccine efficacy in NHPs, including pulmonary pathology score (Fig. 5C), total gross pathology score (Fig. 5D), and chest X ray (Fig. 5E). The levels of pulmonary disease measured by each of these approaches generally agreed and reflected the trends identified by using the quantitative measures. The gross pathology scoring system was able to distinguish between groups of BCG-vaccinated and unvaccinated animals ($P = 0.017$) (Table 2), but there was no difference between BCG-MVA85A-vaccinated and BCG-vaccinated animals and unvaccinated controls using this measure. The pathology scoring system did not predict survival in the BCG-vaccinated group. No significant differences between study groups were seen in terms of chest X-ray score; lung pathology score; bacterial load; or clinical disease measures, weight loss, or ESR (Table 2).

The level of pulmonary disease by all scoring systems also agreed with the level of changes determined by the clinical measures of disease severity at termination, namely, weight loss, decreased erythrocyte hemoglobin concentration, and increase in the ESR, with most changes occurring in the animals with the greatest level of pulmonary disease. Across all animals in the study regardless of treatment grouping, the ratio of lesion volume to lung volume, ESR, and mean cell hemoglobin concentration for animals correlated with survival time after challenge ($P = 0.0267$ for the ratio of lesion volume to lung volume, $P = 0.0038$ for ESR, and $P = 0.0120$ for hemoglobin concentration).

The lung bacterial load tended to be lower in animals that did not show adverse clinical indicators at termination (animals K65, K43, K50, and K59) (Fig. 5H). Extrapulmonary dissemination occurred in all animals in the study, and the pattern of spread to spleen, kidneys, and/or liver did not distinguish between test groups.

IFN-γ response following aerosol challenge with *M. tuberculosis*. The *Mycobacterium*-specific IFN-γ response was measured by an ELISpot assay (Fig. 6A, B, and C) and ELISA (Fig. 6D). A comparison of the responses made by animals in each test group during the first 6 weeks after challenge suggested a trend for an increased frequency of Ag85A-specific and PPD-specific IFN-γ-producing cells in BCG-MVA85A-vaccinated animals (group A) compared to that in the BCG-vaccinated (group B) and the unvaccinated (group C) animals (Fig. 6B and C). The difference in the PPD-specific responses was found to be statistically significant ($P = 0.03$) between the BCG-MVA85A-vaccinated and the unvaccinated animals but not statistically different between the BCG- and the BCG-MVA85A-vaccinated animals. The frequency of ESAT6-specific IFN-γ-producing cells and the quantity of IFN-γ secreted following stimulation with PPD were similar for all the test groups during this initial 6-week period.

Comparison of responses made by animals in the different

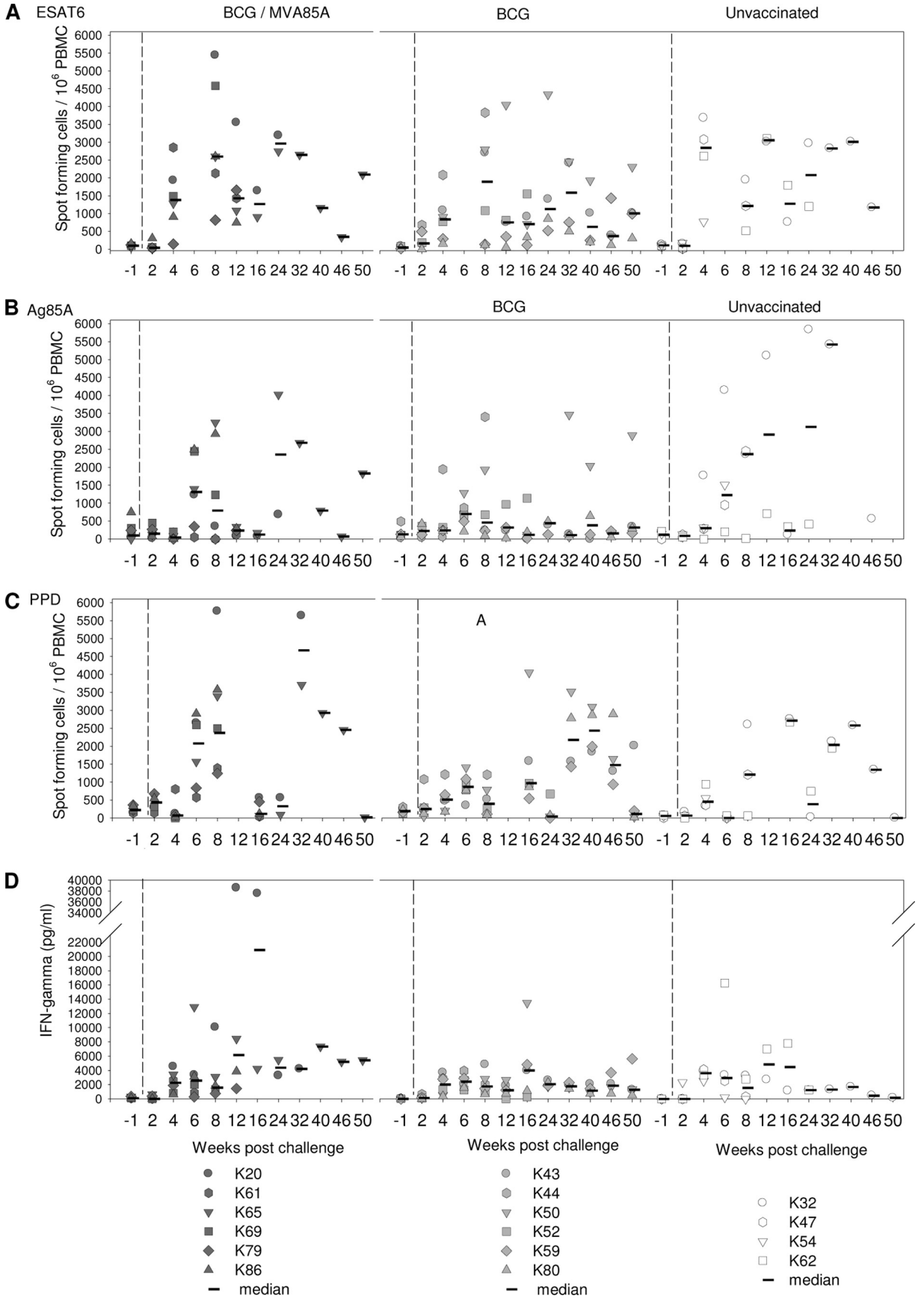

FIG. 6. Immune responses after aerosol challenge with *M. tuberculosis*. (A to C) Frequency of mycobacterium-specific IFN-γ-secreting cells after challenge measured by ELISpot assay. (A) ESAT6; (B) Ag85A; (C) PPD. (D) Profile of IFN-γ secretion by PPD-stimulated whole blood measured by ELISA.

test groups was valid only in the early phase after infection while all animals remained in the study.

Proliferative response following aerosol challenge with *M. tuberculosis*. PPD-specific proliferative responses were detected in five of the six BCG-vaccinated animals (animals K43, K44, K50, K59, and K80), five of the six BCG-MVA85A-vaccinated animals (animals K61, K65, K69, K79, and K86), and one of the unvaccinated animals (animal K32) following infection with *M. tuberculosis.* Responses were generally low (SI < 10), were inconsistent over time, and did not differentiate between vaccine groups or predict progression with disease.

DISCUSSION

There is a growing need for improved preclinical models for vaccine assessment with sensitive and discriminatory readouts that would act as correlates of protection as work continues to develop a new, more-effective TB vaccine. Ideally, models should be highly reproducible, include the same endpoints as those used in human clinical trials, and be validated to predict efficacy in humans. This study developed and characterized an aerosol challenge model of *M. tuberculosis* in rhesus macaques and assessed immunological and clinical readouts for utility in vaccine evaluation studies. Aerosol challenge models have been used previously to evaluate the efficacy of TB vaccines in NHPs (2, 9, 14, 26, 29), but no standardized or validated protocol has emerged. However, it is clear that the disease that develops following low-dose aerosol challenge shows marked animal-to-animal variation, particularly when the readout of disease severity is survival, and much larger group sizes will be required if survival is used as an endpoint in future vaccine evaluation studies. Even more pronounced heterogeneity in progression to disease was observed when very low doses were administered by the intratracheal route, suggesting that the lower the initial inoculum, the less predictable the outcome of the host-pathogen interaction from one animal to the next (8).

Our study is the first example of TB vaccine evaluation in rhesus macaques where long-term survival was one of the primary endpoints. The study was taken to a point where disease progressed in all unvaccinated control animals to allow outcomes in vaccinated animals to be compared by using a variety of pathological and clinical readouts. Previous studies in which TB vaccine candidates have been evaluated for efficacy in rhesus macaques have ended at a fixed point, 8 to 17 weeks after either aerosol (1, 2, 3, 14, 26) or intratracheal (15, 31) challenge. Longer-term studies of vaccine efficacy with postchallenge investigation periods in excess of 16 weeks have been conducted with cynomolgus macaques (22, 23, 25). In the latter studies, survival after challenge has provided a readout of vaccine efficacy, although only one of the four efficacy studies reported (21) was sufficiently long to allow the entire unvaccinated group to progress to end-stage disease, i.e., not survive the challenge. Our study has shown that the heterogeneity in long-term disease progression following relatively low-dose aerosol challenge is not compatible with survival as an endpoint of vaccine efficacy in rhesus macaques.

In NHP vaccine efficacy studies with group sizes of about six animals, as used here, survival appears not to be a reliable endpoint. In this study, the limitation by cost of group size meant that a survival difference between the BCG-vaccinated group and the naïve control group was of borderline statistical significance and dependent on the statistical analysis used. Comparison of the survival time after challenge of BCG-MVA85A-vaccinated animals with those of BCG-vaccinated animals and unvaccinated animals using the Cox regression or the Kaplan-Meier log rank statistical test did not show a statistically significant difference between survival in any of the three experimental groups. The conclusion to be drawn from the current study is that survival does not discriminate between different groups when small numbers of animals are used, and this is supported by a retrospective analysis of numerous guinea pig studies, even though larger group sizes can be more easily achieved for guinea pigs (35). Furthermore, survival is a complex endpoint with many contributing factors implicated. In human efficacy trials, death would not be an endpoint; rather, disease defined by positive culture or presentation of clinical symptoms or signs or abnormal investigations such as a chest radiograph would be used. While animal models provide excellent test systems for the evaluation of new vaccines, there are constraints that prevent these models from simulating every aspect of the natural disease in humans. For example, only a small percentage of humans who are exposed to tuberculosis will get the disease. In animal models, the uniform development of disease within a reasonable time frame after challenge in unvaccinated control groups is essential, as the process of vaccine evaluation relies on the definition of differences in disease burden between vaccinated and unvaccinated animals. These requirements necessitate the use of challenge doses sufficient to ensure uniform disease induction as well as the use of complex readouts.

The evaluation of vaccine efficacy was also shown to be complex and not clear-cut. Other clinical, pathological, and bacteriology-based measures were confounded by groups having a mixture of survivor and nonsurvivor animals. The impact of this is that the animals that reach their humane endpoint will have CFU counts and pathology scores at the maximum for the readouts due to late-stage accelerated bacterial growth and inflammation, whereas survivors will have lower levels. Some readouts (total pathology score, chest radiograph, and bacterial load) showed a reduction in surviving animals but lacked sufficient power to differentiate between study groups. A significantly higher number of lesions was counted for the BCG-vaccinated animals than for the unvaccinated animals. This finding likely reflects difficulties associated with the manual counting of both discrete and coalesced lesions as a readout of disease burden, particularly in animals with more severe disease, where the individual lesions became difficult to distinguish and eventually too numerous to count. The disease in the unvaccinated animals was more severe than that in BCG-vaccinated animals, and a greater proportion of coalescing lesions and consolidated lobes led to an apparently low total lesion count. In contrast, the lesions in the BCG-vaccinated animals tended to be smaller and remained discrete and were therefore more easily countable.

The level of PPD-specific proliferative responses induced by vaccination did not correlate with protection. For example, animal K44 from the BCG-vaccinated group made the largest and most consistent proliferative responses after vaccination and yet was the first animal in this group to reach humane-

endpoint criteria following challenge. Similarly, PPD-specific proliferative responses of a similar magnitude were detected in two animals (animals K65 and K69) in the BCG-MVA85A-vaccinated group 2 weeks after vaccination with MVA85A, but the outcome of *M. tuberculosis* infection was very different. The disease in animal K69 progressed rapidly and met humane-endpoint criteria within 10 weeks of challenge, whereas animal K65 successfully controlled disease for the duration of the study.

IFN-γ is considered to be an essential cytokine for the control of TB. Three assays were used to assess the responses made to vaccination and challenge. These assays were the ELISpot assay used in clinical trials with MVA85A (20) to measure the frequency of IFN-γ-secreting cells, an ELISA to quantify the IFN-γ secreted in response to the antigenic stimulation of whole blood (5), and intracellular cytokine staining followed by flow cytometry. The response profiles of each animal defined by the three approaches showed similar trends, but none of the IFN-γ profiles following vaccination correlated with protection. Interestingly, the animal (animal K65) that showed the highest IFN-γ response, as measured by both an ELISpot assay and ELISA, and a high level of Ag85A-specific polyfunctional $CD4^+$ T cells 1 week after vaccination with MVA85A controlled infection most effectively after challenge, showed fewer clinical symptoms during the postchallenge phase of the study, and had the lowest disease burden when euthanized at the end of the study. During the period after MVA85A boost and prior to challenge, the PPD-specific responses in the group vaccinated with BCG-MVA85A were not significantly different from those seen for the group vaccinated with BCG alone. This is in contrast with BCG-vaccinated mice that were boosted with MVA85A, and this vaccine regimen was shown previously to protect mice against aerosol challenge with *M. tuberculosis* (13). In our study the lack of a post-MVA85A boost response in the other five animals in the BCG-MVA85A-vaccinated group perhaps explains why survival in this group was not improved as reported previously by Verreck et al. (31). However, ELISpot responses induced immediately after the MVA85A boost in the animals in the study reported by Verreck et al. were not measured, and so this cannot be confirmed. Further work is required to understand why the immune response to MVA85A in five of the animals in this study were considerably lower than those seen in humans despite the NHPs in this experiment having received a higher dose of vaccine (20). While a trend for a larger early IFN-γ response in the BCG-MVA85A-vaccinated group was suggested, the validity of a continued comparison of responses later than 8 weeks after challenge was confounded by the loss of some animals from the study. The only readout to reliably distinguish vaccinated and unvaccinated NHPs was MR stereology at the end of the study. The even distribution of pulmonary disease following aerosol challenge reduced the sampling error associated with readouts reliant on sampling less than the entire lung and allowed the successful application of the MR stereology technique without compromising the use of other histopathology-based readouts.

Any long-term study that relies on end-of-study readouts may suffer when data for survivors are combined with data for nonsurvivors. Therefore, longitudinal "in-life" measurements that can include all study subjects are required. "In-life" longitudinal measurements of the immune response were used in this study; however, the currently proposed key markers were not shown to correlate with protection. We conclude that given the lack of statistical power, it is generally not warranted to conduct long-term survival studies on NHPs for ethical and financial reasons, and shorter experiments with defined endpoints are recommended. Radiological imaging offered a reliable correlate even at the end of the study, and work is in progress to investigate the potential of "in-life" imaging as a readout of vaccine efficacy.

ACKNOWLEDGMENTS

This work was supported by the Department of Health, United Kingdom.

The views expressed in this publication are those of the authors and not necessarily those of the Department of Health.

We thank the staff of the Biological Investigations Group at HPA for assistance in conducting studies, Graham Hatch for aerobiology assistance, Nicola Alder for statistical support, Arturo Reyes-Sandoval for the staining panel used for polyfunctional T-cell analysis, and Susan Gray for histology support.

REFERENCES

1. **Anacker, R. L., W. Brehmer, W. R. Barclay, W. R. Leif, E. Ribi, J. H. Simmons, and A. W. Smith.** 1972. Superiority of intravenously administered BCG and BCG cell walls in protecting rhesus monkeys (*Macaca mulatta*) against airborne tuberculosis. Z. Immunitatsforsch. Exp. Klin. Immunol. **143:**363–376.
2. **Barclay, W. R., R. L. Anacker, W. Brehmer, W. Leif, and E. Ribi.** 1970. Aerosol-induced tuberculosis in subhuman primates and the course of the disease after intravenous BCG vaccination. Infect. Immun. **2:**574–582.
3. **Barclay, W. R., W. M. Busey, D. W. Dalgard, R. C. Good, B. W. Janicki, J. E. Kasik, E. Ribi, C. E. Ulrich, and E. Wolinsky.** 1973. Protection of monkeys against airborne tuberculosis by aerosol vaccination with bacillus Calmette-Guerin. Am. Rev. Respir. Dis. **107:**351–358.
4. **Basaraba, R. J.** 2008. Experimental tuberculosis: the role of comparative pathology in the discovery of improved tuberculosis treatment strategies. Tuberculosis (Edinb.) **88**(Suppl. 1)**:**S35–S47.
5. **Black, G. F., P. E. M. Fine, D. K. Warndorff, S. Floyd, R. E. Weir, J. M. Blackwell, L. Bliss, L. Sichali, L. Mwaungulu, S. Chaguluka, E. Jarman, B. Ngwira, and H. M. Dockrell.** 2001. Relationship between IFN-gamma and skin test responsiveness to *Mycobacterium tuberculosis* PPD in healthy, non-BCG-vaccinated young adults in Northern Malawi. Int. J. Tuber. Lung Dis. **5:**664–672.
6. **Beveridge, N. E., D. A. Price, J. P. Casazza, A. A. Pathan, C. R. Sander, T. E. Asher, D. R. Ambrozak, M. L. Precopio, P. Scheinberg, N. C. Alder, M. Roederer, R. A. Koup, D. C. Douek, A. V. Hill, and H. McShane.** 2007. Immunisation with BCG and recombinant MVA85A induces long-lasting, polyfunctional *Mycobacterium tuberculosis*-specific CD4+ memory T lymphocyte populations. Eur. J. Immunol. **37:**3089–3100.
7. **Blanchard, T. J., A. Alcami, P. Andrea, and G. L. Smith.** 1998. Modified vaccinia virus Ankara undergoes limited replication in human cells and lacks several immunomodulatory proteins: implications for use as a human vaccine. J. Gen. Virol. **79:**1159–1167.
8. **Capuano, S. V., D. A. Croix, S. Pawar, A. Zinovik, A. Myers, P. L. Lin, S. Bissel, C. Fuhrman, E. Klein, and J. A. Flynn.** 2003. Experimental *Mycobacterium tuberculosis* infection of cynomolgus macaques closely resembles the various manifestations of human *M. tuberculosis* infection. Infect. Immun. **71:**5831–5844.
9. **Chaparas, S. D., R. C. Good, and B. W. Janicki.** 1975. Tuberculin-induced lymphocyte transformation and skin reactivity in monkeys vaccinated or not vaccinated with bacille Calmette-Guerin, then challenged with virulent *Mycobacterium tuberculosis*. Am. Rev. Respir. Dis. **112:**43–47.
10. **Colditz, G. A., T. F. Brewer, C. S. Berkey, M. E. Wilson, E. Burdick, H. V. Fineberg, and F. Mosteller.** 1994. Efficacy of BCG vaccine in the prevention of tuberculosis. Meta-analysis of the published literature. JAMA **271:**698–702.
11. **Druett, H. A.** 1969. A mobile form of the Henderson apparatus. J. Hyg. (Lond.) **67:**437–448.
12. **Good, R. C.** 1968. Simian tuberculosis: immunologic aspects. Ann. N. Y. Acad. Sci. **154:**200–213.
13. **Goonetilleke, N. P., H. McShane, C. M. Hannan, R. J. Anderson, R. H. Brookes, and A. V. Hill.** 2003. Enhanced immunogenicity and protective efficacy against Mycobacterium tuberculosis of bacille Calmette-Guérin vaccine using mucosal administration and boosting with a recombinant modified vaccinia virus Ankara. J. Immunol. **171:**1602–1609.

14. **Janicki, B. W., R. C. Good, P. Minden, L. F. Affronti, and W. F. Hymes.** 1973. Immune responses in rhesus monkeys after bacille Calmette-Guerin vaccination and aerosol challenge with *Mycobacterium tuberculosis*. Am. Rev. Respir. Dis. **107:**359–366.
15. **Langermans, J. A. M., P. Anderson, D. van Soolingen, R. A. W. Verenne, P. A. Frost, T. van der Laan, S. Kroon, I. Peekel, S. Florquin, and A. W. Thomas.** 2000. Divergent effect of bacillus Calmette-Guerin (BCG) vaccination on *Mycobacterium tuberculosis* infection in highly related macaque species: implications for primate models in tuberculosis vaccine research. Proc. Natl. Acad. Sci. U. S. A. **98:**11497–11502.
16. **Lin, P. L., S. Pawar, A. Myers, A. Pergu, C. Fuhrman, T. A. Reinhart, S. V. Capuano, E. Klein, and J. L. Flynn.** 2006. Early events in *Mycobacterium tuberculosis* infection in cynomolgus macaques. Infect. Immun. **74:**3790–3803.
17. **McMurray, D. N., F. M. Collins, A. M. Dannenberg, Jr., and D. W. Smith.** 1996. Pathogenesis of experimental tuberculosis in animal models. Curr. Top. Microbiol. Immunol. **215:**157–179.
18. **McMurray, D. N.** 2000. A non-human primate model for the preclinical testing of new tuberculosis vaccines. Clin. Infect. Dis. **30**(Suppl. 3)**:**S210–S212.
19. **McShane, H., R. Brookes, S. C. Gilbert, and A. V. Hill.** 2001. Enhanced immunogenicity of CD4(+) T-cell responses and protective efficacy of a DNA-modified vaccinia virus Ankara prime-boost vaccination regimen for murine tuberculosis. Infect. Immun. **69:**681–686.
20. **McShane, H., A. A. Pathan, C. R. Sander, S. M. Keating, S. C. Gilbert, K. Huygen, H. A. Fletcher, and A. V. Hill.** 2004. Recombinant modified vaccinia virus Ankara expressing antigen 85A boosts BCG-primed and naturally acquired antimycobacterial immunity in humans. Nat. Med. **10:**1240–1244.
21. **Pathan, A. A., C. R. Sander, H. A. Fletcher, I. Poulton, N. C. Alder, A. V. Hill, and H. McShane.** 2007. Safety and immunogenicity of boosting BCG vaccinated subjects with BCG: comparison with boosting with a new TB vaccine, MVA85A. PLoS One **2:**e1052.
22. **Okada, M., Y. Kita, T. Nakajima, N. Kanamaru, S. Hashimoto, T. Nagasawa, Y. Kaneda, S. Yoshida, Y. Nishida, H. Nakatani, K. Takao, C. Kishigami, Y. Inoue, M. Matsumoto, D. N. McMurray, E. C. Dela Cruz, E. V. Tan, R. M. Abalos, J. A. Burgos, P. Saunderson, and M. Sakatani.** 2009. Novel prophylactic and therapeutic vaccine against tuberculosis. Vaccine **26:**3267–3270. [Epub ahead of print.]
23. **Okada, M., Y. Kita, T. Nakajima, N. Kanamaru, S. Hashimoto, T. Nagasawa, Y. Kaneda, S. Yoshida, Y. Nishida, R. Fukamizu, Y. Tsunai, R. Inoue, H. Nakatani, Y. Namie, J. Yamada, K. Takao, R. Asai, R. Asaki, M. Matsumoto, D. N. McMurray, E. C. Dela Cruz, E. V. Tan, R. M. Abalos, J. A. Burgos, R. Gelber, and M. Sakatani.** 2007. Evaluation of a novel vaccine (HVJ-liposome/HSP65 DNA+IL-12 DNA) against tuberculosis using the cynomolgus monkey model of TB. Vaccine **20:**2990–2993.
24. **Orme, I. M., D. N. McMurray, and J. T. Belisle.** 2001. Tuberculosis vaccine development: recent progress. Trends Microbiol. **9:**115–118.
25. **Reed, S. G., R. N. Coler, W. Dalemans, E. V. Tan, E. C. Dela Cruz, R. J. Basaraba, I. M. Orme, Y. A. W. Skeiky, M. R. Alderson, K. D. Cowgill, J.-P. Prieels, R. M. Abalos, M.-C. Dubois, J. Cohen, P. Mettens, and Y. Lobet.** 2009. Defined tuberculosis vaccine, Mtb72F/AS02A, evidence of protection in cynomolgus monkeys. Proc. Natl. Acad. Sci. U. S. A. **106:**2301–2306.
26. **Ribi, E., R. L. Anacker, W. R. Barclay, W. Brehmer, S. C. Harris, W. R. Leif, and J. Simmons.** 1971. Efficacy of mycobacterial cell walls as a vaccine against airborne tuberculosis in the rhesus monkey. J. Infect. Dis. **123:**527–538.
27. **Rodrigues, L. C., V. K. Diwan, and J. G. Wheeler.** 1993. Protective effect of BCG against tuberculous meningitis and miliary tuberculosis: a meta-analysis. Int. J. Epidemiol. **22:**1154–1158.
28. **Sharpe, S. A., E. Eschelbach, R. J. Basaraba, F. Gleeson, G. A. Hall, A. McIntyre, A. Williams, S. L. Kraft, S. Clark, K. Gooch, G. Hatch, I. M. Orme, P. D. Marsh, and M. J. Dennis.** 2009. Determination of lesion volume by MRI and stereology in a macaque model of tuberculosis. Tuberculosis **89:**405–416. [Epub ahead of print.]
29. **Shen, Y., D. Zhou, L. Qiu, X. Lai, M. Simon, L. Shen, Z. Kou, Q. Wang, L. Jiang, J. Estep, R. Hunt, M. Clagett, P. K. Sehgal, Y. Li, X. Zeng, C. T. Morita, M. B. Brenner, N. L. Letvin, and Z. W. Chen.** 2002. Adaptive immune responses of Vγ2Vδ2+ T cells during mycobacterial infections. Science **295:**2255–2258.
30. **Trunz, B. B., P. Fine, and C. Dye.** 2006. Effect of BCG vaccination on childhood tuberculous meningitis and miliary tuberculosis worldwide: a meta-analysis and assessment of cost-effectiveness. Lancet **367:**1173–1180.
31. **Verreck, F. A. W., R. A. W. Ververne, I. Kondova, K. W. van Kralingen, E. J. Remarque, G. Braskamp, N. M. van der Werff, A. Kersbergen, T. H. M. Ottenhoff, P. J. Heidt, S. C. Gilbert, B. Gicquel, A. V. S. Hill, C. Martin, H. McShane, and A. W. Thomas.** 2009. MVA.85A boosting of BCG and an attenuated *phoP* deficient *M. tuberculosis* vaccine both show protective efficacy against tuberculosis in rhesus macaques. PLoS One **4:**e5264.
32. **Vordermeier, H. M., S. G. Rhodes, G. Dean, N. Goonetilleke, K. Huygen, A. V. Hill, R. G. Hewinson, and S. C. Gilbert.** 2004. Cellular immune responses induced in cattle by heterologous prime-boost vaccination using recombinant viruses and bacille Calmette-Guérin. Immunology **112:**461–470.
33. **Vordermeier, H. M., B. Villarreal-Ramos, P. J. Cockle, M. McAulay, S. G. Rhodes, T. Thacker, S. C. Gilbert, H. McShane, A. V. Hill, Z. Xing, and R. G. Hewinson.** 2009. Viral booster vaccines improve Mycobacterium bovis BCG-induced protection against bovine tuberculosis. Infect. Immun. **77:**3364–3373.
34. **Williams, A., N. P. Goonetilleke, H. McShane, S. O. Clark, G. Hatch, S. C. Gilbert, and A. V. Hill.** 2005. Boosting with poxviruses enhances *Mycobacterium bovis* BCG efficacy against tuberculosis in guinea pigs. Infect. Immun. **73:**3814–3816.
35. **Williams, A., Y. Hall, and I. M. Orme.** 2009. Evaluation of new vaccines for tuberculosis in the guinea pig model. Tuberculosis (Edinb.) **89:**389–397. [Epub ahead of print.]
36. **WHO.** 2008. Global tuberculosis control: surveillance, planning, financing. WHO report. WHO/htm/TB/2008.393. WHO, Geneva, Switzerland.